Journal of Inflammation Research

Dovepress
open access to scientific and medical research

Open Access Full Text Article

ORIGINAL RESEARCH

Multi-Omics Analysis and Verification of the Oncogenic Value of CCT8 in Pan-Cancers

Lian Gong[1], Ming Zhong[2], Kai Gong[3], Zhanwang Wang[1], Yong Zhong[4], Yi Jin[1], Haotian Chen[1], Panpan Tai[1], Xinyu Chen[1], Aiyan Chen[1], Ke Cao[1]

[1]Department of Oncology, Third Xiangya Hospital, Central South University, Changsha, 410013, People's Republic of China; [2]Department of Nephrology, Center of Kidney and Urology, the Seventh Affiliated Hospital, Sun Yat-sen University, Shenzhen, People's Republic of China; [3]Department of Clinical Medicine, Xiangnan University, Chenzhou, People's Republic of China; [4]Department of Clinical Medicine, Hubei Enshi College, Enshi, People's Republic of China

Correspondence: Ke Cao, Email csucaoke@163.com

Background: Chaperonin-containing TCP1 subunit 8 (CCT8) has been proved to be involved in the occurrence and development of some cancers. However, no study has reported the potential role of CCT8 in a pan-cancer manner.

Methods: TIMER2.0, GEPIA2, UALCAN and Sangerbox were used to explore the expression, prognosis and methylation of CCT8. We used cBioPortal, TISIDB, SangerBox, TIMER2.0 and TISMO to investigate the genetic alteration of CCT8 and the relationship of CCT8 with molecular subtype, immune subtype, immune infiltration and immunotherapy response. CCT8-related genes were screened out through GEPIA and STRING for Gene Ontology (GO) and Kyoto Encyclopedia of Genes and Genomes (KEGG) enrichment analysis. CCK-8, the colony formation assay, the wound healing assay and the Transwell assay were performed to explore the influence of CCT8 on proliferation and migration.

Results: CCT8 was highly expressed in most cancers with a poor prognosis. The expression level of CCT8, which was affected by the promoter region methylation and genetic alteration, was related to the molecular and immune subtype of cancers. Interestingly, CCT8 was positively associated with the activated CD4 T cells and type 2 T-helper cells. CCT8 played a vital role in the cell cycle and RNA transport of cancers, and it significantly inhibited the proliferation and migration of lung adenocarcinoma cells when it was knocked down.

Conclusion: CCT8 plays an indispensable role in promoting the proliferation and migration of many cancers. CCT8 might be a biomarker of T-helper type 2 (Th2) cell infiltration and a promising therapeutic target for T-helper type 1(Th1)/Th2 imbalance.

Keywords: CCT8, survival, immune infiltration, biomarker, pan-cancer

Introduction

Cancer is a complex disease initiated by endogenous and exogenous factors, such as environmental, genetic and immune factors. With the advancement of bioinformatics analysis based on public cancer datasets, we can explore the general mechanism of oncogenes or tumor suppressor genes in tumorigenesis and development in a pan-cancer manner, which can provide possible targets for cancer treatment.[1]

The cytoplasmic chaperonin-containing TCP1 complex (CCT), also called the TCP1 ring complex (TRiC), comprises two identical rings.[2] Each ring consists of eight different CCTs, CCT1-CCT8. The TRiC plays a vital role in maintaining cell homeostasis by helping to fold numerous proteins, including actin and tubulin, etc. CCT8, a subunit of the TRiC, has been proved to promote malignant tumor progression in colorectal cancer, liver cancer, brain glioma and esophageal squamous cell carcinoma.[2–5] However, there has been no systematic study on CCT8 in a pan-cancer manner.

We comprehensively analyzed the gene expression, survival, methylation, genetic alteration and immune infiltration of CCT8 in a pan-cancer manner.[6] We performed GO and KEGG analysis on related genes and carried out in vitro cell experiments to explore the potential role and molecular mechanism of CCT8 in different cancers. Our study aimed to explore the role and mechanism of CCT8 in human cancer, so as to provide insights for new anti-tumor strategies.

Received: 3 January 2023
Accepted: 6 April 2023
Published: 29 May 2023

Materials and Methods

Expression Analysis

We used TIMER2.0 (http://timer.cistrome.org/) to explore CCT8's mRNA expression in different cancers and normal tissues of The Cancer Genome Atlas (TCGA).[7] UALCAN (http://ualcan.path.uab.edu/) provided protein expression analysis using data from the Clinical Proteomic Tumor Analysis Consortium (CPTAC) and the International Cancer Proteogenome Consortium (ICPC) datasets.[8,9] We used GEPIA (http://gepia.cancer-pku.cn/) to compare CCT8 expression in several cancer types based on TCGA and The Genotype-Tissue Expression (GTEx).[10,11] The Human Protein Atlas (https://www.proteinatlas.org/) was consulted to determine the immunohistochemistry of CCT8 in cancer and normal tissues.[12] The CCLE was a high-throughput web-based tool with large numbers of human cancer cell lines and unique datasets. We downloaded the gene expression data of different tumor cell lines from the CCLE database, and explored the expression level of CCT8 in different tumors by.[13–15]

Survival Analysis

Sangerbox3.0 (http://vip.sangerbox.com/login.html) was used to establish the Cox proportional hazards regression model by using the coxph function of the R software package survival (version 3.2–7) to analyze the relationship between gene expression and prognosis in each tumor, and we used the Log rank test to perform statistical tests to obtain prognostic significance. GEPIA performed overall survival (OS), disease-specific survival (DSS), disease-free interval (DFI) and progression-free interval (PFI) analysis based on CCT8 expression. GEPIA used the Log rank test for the hypothesis test. The group cutoff was adjusted to the median. GEPIA also generated expression plots on the basis of patient pathological stage. One-way ANOVA was used for differential gene expression analysis, and pathological stage was used as a variable to calculate differential expression.

Promoter Methylation and Genetic Alteration Analysis

UALCAN assessed differences in methylation levels in the CCT8 promoter region between normal and cancer samples. MethSurv (https://biit.cs.ut.ee/methsurv/) is a web tool for survival analysis based on CpG methylation patterns. We used it to explore the prognostic impact of CCT8 methylation on different tumors.[16–18] The cBioPortal tool (https://www.cbioportal.org/) was used to analyze alteration frequency across all TCGA tumors. On the cBioPortal website, "TCGA Pan Cancer Atlas Studies" can be selected to find the gene alteration profile of CCT8 in all TCGA tumors; in this way, we obtained alteration frequency, mutation type and copy number alteration (CNA) results.[7] Sangerbox3.0 was used to investigate the effect of single-nucleotide variants (SNVs) and copy number variation (CNV) on CCT8 expression in different cancers.

Molecular Subtype, Immune Subtype, Immune Infiltration and Immunotherapy

TISIDB (http://cis.hku.hk/TISIDB/index.php) investigated CCT8 expression in cancer-immune and molecular subtypes. Sangerbox was applied to survey the association between CCT8 expression and ESTIMATEScore, as well as the relationship between tumor-infiltrating immune cells (TIICs).[7,19] Then, we used Sangerbox3.0 to investigate the relationship between CCT8 expression and classical immune checkpoints, as well as microsatellite instability (MSI), neoantigen and tumor mutation burden (TMB). We utilized the "Immune-Gene" module of TIMER2.0 to investigate the association between CCT8 and details of CD4+ T-immune cell infiltration in various TCGA cancers. TISMO (http://tismo.cistrome.org) was used to assess the ability of CCT8 to predict immunotherapy response in mouse immunotherapy cohorts and tumor cell lines.[8]

Connectivity Map Specific Inhibitor Analysis

The Connectivity Map (CMap) can be used to reveal the functional linkages of small molecule compounds, genes and disease states.[12,20–22] We divided each tumor into high and low expression groups according to the expression level of CCT8, and performed differential analysis to obtain differential genes. We download experimental data from the CMap (https://portals.broadinstitute.org/cmap/) database. Then, we calculated compound scores for each tumor using R (UCS and UVM had few differential genes, so we did not perform subsequent drug score calculations).

Enrichment Analysis of CCT8-Related Genes

We applied the "Similar Genes Detection" module in GEPIA to identify 100 genes with similar expression patterns to CCT8 based on all the TCGA tumors.[7] Then, we used the Pearson method to perform pair-wise gene expression correlation analysis for given sets of TCGA expression data. STRING (https://string-db.org/) was used to construct functional protein association networks. The basic settings were as follows: network type: physical subnetwork; active interaction sources: experiments; minimum required interaction score: medium confidence (0.400); max number of interactors showing: 1st shell and no more than 50 interactors. We applied the "tidyr" and "ggplot2" R packages to visualize enrichment pathways. R software (R-4.0.2, 64-bit) (https://www.r-project.org/) was applied in our study.

Cell Line Culture and siRNA Delivery

The lung adenocarcinoma cell line A549 was purchased from the Cell Bank of Type Culture Collection, Chinese Academy of Science (Shanghai, China), and cultured in a 37°C incubator using 1640 medium supplemented with 10% fetal bovine serum (FBS) and 1% penicillin–streptomycin solution. The siCCT8s for knockdown CCT8 were purchased from GenePharma (Shanghai, China) and transfected with Lipofectamine™ 2000 reagent (Invitrogen, Shanghai, China). A549 cells were seeded in 6-well plates the day before transfection. After 5 μL of Lipofectamine™ 2000 and 100 pmol siRNA were mixed with 250ul Opti-men separately in two EP tubes for 5 minutes, the two were mixed and allowed to stand for 15 minutes. Then, the mixture was added to the cells for transfection. The cells were changed into whole culture medium 24 hours after transfection. After 48 hours, the cells were collected for RT-qPCR to detect CCT8 knockdown efficiency or for proliferation and migration experiments. The siRNA sequences were as follows: siCCT8#1, sense 5'-GCUCAUGAGAUUCUUCCUATT-3'sense, antisense 5'- UAGGAAGAAUCUCAUGAGCTT-3'; siCCT8#2, sense 5'-ACUCAAGAAUCACCUGAUGTT-3', antisense 5'-CAUCAGGUGAUUCUUGAGUTT-3'; negative control (NC), sense 5'-UUCUCCGAACGUGUCACGUTT-3', antisense 5'-ACGUGACACGUUCGGAGAATT-3'.

RNA Isolation and Quantitative Real-time PCR (qRT-PCR)

The total RNA was extracted with RNA fast200 (Fijie Reagent, Shanghai, China) according to the instructions. Vazyme reagent (Nanjing, China) was used for synthesizing cDNA and qPCR according to the instructions. GAPDH was applied as an internal control. The qRT-PCR primers were as follows: GAPDH, forward 5'-GTCAGCCGCATCTTCTTT −3', reverse 5'-CGCCCAATACGACCAAAT −3'; CCT8, forward 5'- GGAGGGAGCGAAACACTTTT-3', reverse 5'-TTGCAGCAGGATGCTGTACT-3'. The $2^{-\Delta\Delta Ct}$ method was used to quantify the gene expression level.

CCK-8 Assay

The CCK-8 Kit was purchased from bioshar (Anhui, China). We Seeded 2000 cells per well to 96-well plates after transfection according to experimental requirements, with 3 complex wells per set. Testing started 24 hours later and continued for 4 days (0, 1, 2, 3). The culture medium was soaked and discarded. Then, CCK-8 reagent was mixed with the culture medium at a ratio of 1:10, and 110ul of mixed solution was added to each well. After incubation at 37 °C for 1.5h, the OD value at the 450 wavelength was detected on the microplate.

Colony Formation Assay

A549 cells transfected with siRNA for 24 h were seeded into 6-well plates at a density of 1000 per well and cultured for 7–14 days until a cell colony had formed. After the formation of cell clones, the cells were washed once with PBS, fixed with 1mL/well 4% polyoxymethylene for 30 minutes, stained with 1% crystal violet for 10 minutes, and photographed, counted and statistically analyzed after drying.

Wound Healing Assay

A549 cells were seeded in 6-well plates at a density of 2.5×10^5 cells per well, and then the siCCT8#1, siCCT8#2, or siNC were transfected into cells according to the aforementioned siRNA delivery method. After the cells cover the 6-well

plate, we scraped off the cells with a 200 μL pipette tip and changed the medium to serum-free medium, and took images at 0 h, 24 h and 48 h under an inverted microscope.

Transwell Assay

A total of 200ul of cell suspension was inoculated at a cell density of 5×10^5/mL without FBS medium into the upper chamber, and 600 μL of medium containing 20% FBS was added to the lower chamber. After 24 h, cells were fixed with paraformaldehyde and stained with crystal violet. The cells in the upper chamber were wiped off, and the images were collected under a microscope. The number of cells passing through the upper chamber was counted in four random fields under the microscope.

Statistical Analysis

GraphPad Prism 9 and R software (version 4.0.3) was employed for mapping and statistical analysis. Continuous normally distributed variables were shown as mean±standard deviation and compared using one-way ANOVA. $p<0.05$ was considered statistically significant.

Results

CCT8 Expression Analysis

In this study, we used a Wilcoxon test on TIMER2 to analyze CCT8 mRNA expression in tumors, using data from TCGA. The results showed that CCT8 was more highly expressed in 15 cancers than in adjacent tissues, including bladder urothelial carcinoma (BLCA), breast invasive carcinoma (BRCA), cervical squamous cell carcinoma and endocervical adenocarcinoma (CESC), cholangiocarcinoma (CHOL), colon adenocarcinoma (COAD), esophageal carcinoma (ESCA), head and neck squamous cell carcinoma (HNSC), liver hepatocellular carcinoma (LIHC), lung adenocarcinoma (LUAD), lung squamous cell carcinoma (LUSC), prostate adenocarcinoma (PRAD), rectum adenocarcinoma (READ), stomach adenocarcinoma (STAD), thyroid carcinoma (THCA) and uterine corpus endometrial carcinoma (UCEC). It had a lower expression in kidney chromophobe (KICH) and pheochromocytoma and paraganglioma (PCPG) (Figure 1A). Paired sample analysis also suggested that CCT8 was highly expressed in BLCA, BRCA, CHOL, COAD, ESCA, HNSC, KICH, kidney renal clear cell carcinoma (KIRC), kidney renal papillary cell carcinoma (KIRP), LIHC, LUAD, LUSC, PRAD, READ, STAD, THCA and UCEC (Figure 1B). TCGA and GTEx data analysis by Gepia revealed that in CHOL, COAD, lymphoid neoplasm diffuse large B-cell lymphoma (DLBC), READ, testicular germ cell tumors (TGCTs), thymoma (THYM) and uterine carcinosarcoma (UCS), CCT8 expression was higher than in adjacent tissues (Figure 1C). UALCAN provided CCT8 protein expression from the CPTAC and ICPC datasets, confirming that CCT8 protein is highly expressed in COAD, ovarian serous cystadenocarcinoma (OV), ccRCC, UCEC, LC and head and neck cancer, and lowly expressed in BRCA, pancreatic cancer and glioblastoma (Figure 1D). Additionally, boxplot showing the expression levels of CCT8 in different tumor cell lines (Supplementary Figure 1A). The human protein atlas website suggested that CCT8 was high expressed in COAD, LUAD, LUSC, READ, CESC and low expressed in Pancreatic adenocarcinoma (PAAD) (Supplementary Figure 1B). The above results showed that CCT8 was high expressed in most malignant tumors.

CCT8 Survival Analysis

We used the Log rank test in Sangerbox to evaluate the associations between CCT8 and survival outcome with respect to the disease-free interval (DFI) (Figure 2A) and progression-free interval (PFI) (Figure 2B). It was found that eight cancers with high CCT8 expression had a poor DFI: TCGA-BRCA (N=904, p=0.03, HR=1.56 (1.05, 2.31)), TCGA-CESC (N=171, p=0.02, HR=3.26 (1.28, 8.29)), TCGA-KIRP (N=177, p=0.02, HR=2.84 (1.20, 6.68)), TCGA-KIPAN (N=319, p=0.01, HR=1.97 (1.14, 3.40)), TCGA-LIHC (N=294, p=0.01, HR=1.47 (1.09, 1.97)), TCGA-PCPG (N=152, p=0.04, HR=50.67 (0.96, 2681.23)), TCGA-ACC (N=44, p=0.02, HR=2.82 (1.11, 7.12)) and TCGA-MESO (N=14, p=0.04, HR=116.45 (0.97, 13989.59)). Three cancers with low CCT8 expression had a poor DFI: (TCGA-STAD (N=232, p=0.03, HR=0.56 (0.34, 0.94)), TCGA-LGG (N=126, p=0.04, HR=0.26 (0.07, 0.95)) and TCGA-GBMLGG (N=127,

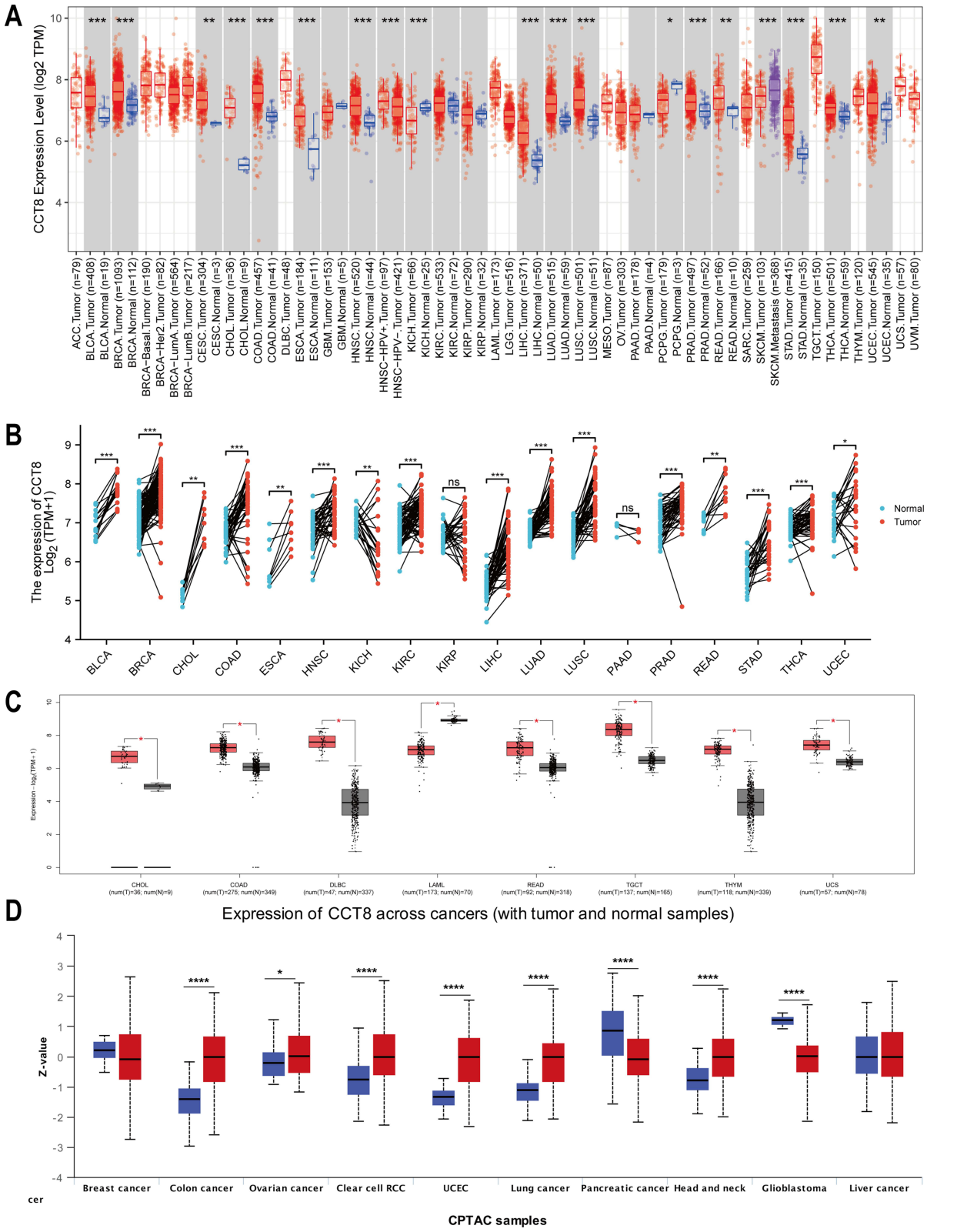

Figure 1 CCT8 expression in tumor and normal tissues. (**A**) Differential expression analysis of CCT8 in TCGA data was analyzed via TIMER2. (**B**) Paired sample analysis showed the expression of CCT8. (**C**) Gepia revealed CCT8 expression in TCGA+GTEx data. (**D**) UALCAN provided CCT8 protein expression from CPTAC and ICPC datasets. In the above four figures, the red represented the tumor tissue, and blue or grey represented the adjacent tissue. The Wilcoxon test was used for the above analysis (*p < 0.05; **p < 0.01; ***p < 0.001; ****p < 0.001).

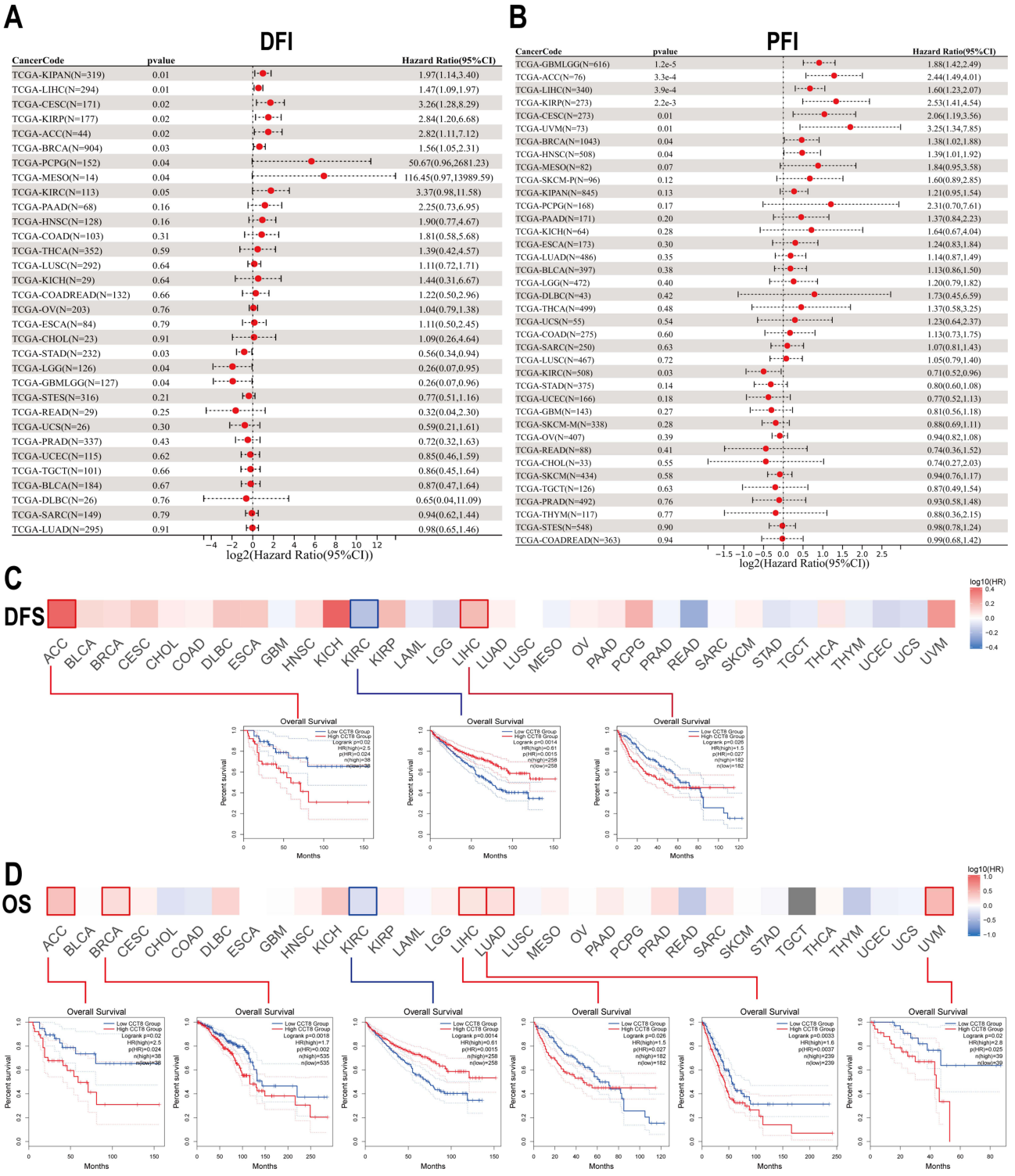

Figure 2 CCT8 expression affected tumor survival. (**A** and **B**) Sangerbox was used to evaluate the associations between CCT8 and survival (DFI (**A**) and PFI (**B**)). (**C** and **D**) GEPIA was used to perform OS (**C**) or DFS (**D**) analysis based on CCT8 expression. In the (**C** and **D**), red and blue represented the high and low CCT8 groups, respectively. The ordinate represented the percent survival, and the abscissa represented the survival time. The Log rank test was used for the above analysis.

p=0.04, HR=0.26 (0.07, 0.96)). We also found that eight cancers with high CCT8 expression had a poor PFI: (TCGA-GBMLGG (p=1.2e-5, HR=1.88 (1.42, 2.49)), TCGA-CESC (p=0.01, HR=2.06 (1.19, 3.56)), TCGA-BRCA (p=0.04, HR=1.38 (1.02, 1.88)), TCGA-KIRP (p=2.2e-3, HR=2.53 (1.41, 4.54)), TCGA-HNSC (p=0.04, HR=1.39 (1.01, 1.92)), TCGA-LIHC (p=3.9e-4, HR=1.60 (1.23, 2.07)), TCGA-UVM (p=0.01, HR=3.25 (1.34, 7.85)) and TCGA-ACC (p=3.3e-

4, HR=2.44 (1.49, 4.01)). Furthermore, KIRC with low CCT8 expression had a poor PFI (TCGA-KIRC (N=508, p=0.03, HR=0.71 (0.52, 0.96))). Sangerbox was used to analyze the impact of CCT8 on overall survival (OS) and disease-specific survival (DSS) (Supplementary Figure 2A and B). The result showed that eight cancers with high CCT8 expression and one cancers with low CCT8 expression had poor OS. It was also found that eleven cancers with high CCT8 expression and one cancer with low CCT8 expression had poor DSS.

We further used GEPIA to perform OS or disease-free survival (DFS) analysis based on CCT8 expression. It was found that high CCT8 expression in adrenocortical carcinoma (ACC) and LIHC was associated with shorter DFS, while KIRC showed the opposite trend (Figure 2C). High CCT8 expression in ACC, BRCA, LIHC, LUAD and uveal melanoma (UVM) predicated shorter OS, while high CCT8 expression in KIRC was associated with longer OS (Figure 2D). Gepia was used to generate CCT8 expression plots on the basis of patient pathological stage, which suggested that CCT8 expression levels in ESCA, LIHC and LUAD were higher in the middle and late stages than in the early stage, while CCT8 expression levels in TGCT were higher in the early stage than in the middle and late stage (Supplementary Figure 2C).

Promoter Methylation and Genetic Alteration Analysis

ULCAN was used to explore the promoter region methylation of CCT8. It was found that the promoter methylation level of CCT8 in BLCA, COAD, HNSC, KIRP, LIHC, LUAD, PRAD, THCA and UCEC was lower than that in adjacent tissues, while the CCT8 promoter region had higher levels of methylation in sarcoma (SARC) (Figure 3A). The most common function of DNA methylation is to inactivate transcription,[23] suggesting that the reduced levels of methylation in the promoter region of CCT8 might be a main cause of the up-regulation of CCT8 in cancers. We further used MethSurv to analyze the effect of CCT8 methylation on survival prognosis in various cancers. The results suggested that cg23817292 was the most common single CpG methylation of CCT8 in 25 cancers (Supplementary Figure 3). Survival analysis showed that high methylation level of CCT8 at cg23817292 site was significantly associated with better prognosis in BLCA, LUSC, STAD, CESC and ESCA. However, it was associated with worse prognosis in SARC and LIHC (Figure 3B).

CCT8 genetic alteration analysis in TCGA cancers was conducted using cBioPortal (Figure 4A). CCT8 genetic alteration was found in esophagogastric adenocarcinoma, ocular melanoma, endometrial carcinoma, sarcoma, cervical adenocarcinoma, bladder urothelial carcinoma, melanoma, invasive breast carcinoma, ovarian epithelial tumor, non-small -cell lung cancer, esophageal squamous cell carcinoma, prostate adenocarcinoma, cervical squamous cell carcinoma, renal clear cell carcinoma, pancreatic adenocarcinoma, colorectal adenocarcinoma leukemia, diffuse glioma, hepatocellular carcinoma and head and neck squamous cell carcinoma. The genetic alteration frequency of esophagogastric adenocarcinoma was the highest (approximately 2.5%), and the main types of genetic alteration were mutation and deep deletion. Analysis of the effect of mutations on prognosis indicated that the LUAD-altered group had a good prognosis, while the BRCA-altered and PRAD-altered groups had a poor prognosis (Supplementary Figure 4).

Sangerbox was used to analyze the effect of SNV on CCT8 expression. We found that CCT8 expression in the mutant group was higher than that in the wild-type group in STES and STAD (Figure 4B). We further analyzed the influence of CNV on CCT8 expression (Figure 4C). It was found that gain group with the highest CCT8 expression and loss group with the lowest CCT8 expression in CESC, LUAD, COAD, READ, BRCA, SARC, STAD, LUSC, OV, and BLCA.CCT8 expression was lower in the gain group than in the neutral group in CESC, LUAD, COAD, READ, BRCA, SARC, STAD, LUSC, OV and BLCA.

Molecular Subtype and Immune Subtype

TISIDB showed significant differences in CCT8 expression among different molecular subtypes in multiple tumors, including BRCA, ESCA, HNSC, KIRP, brain lower-grade glioma (LGG), LIHC, LUSC, OV, PRAD, SKCM, STAD and UCEC (Figure 5 and Supplementary Figure 5). There were significant differences in CCT8 expression among the six immune subtypes of various cancers, including BLCA, BRCA, COAD, HNSC, KIRC, KIRP, LGG, LIHC, LUAD, LUSC, PAAD, PRAD, READ, SARC, STAD and UCEC (Supplementary Figure 6). CCT8 was lowly expressed in the C3 subtype with the best prognosis in most tumors, which indicates that CCT8 might affect the immune infiltration of cancers.

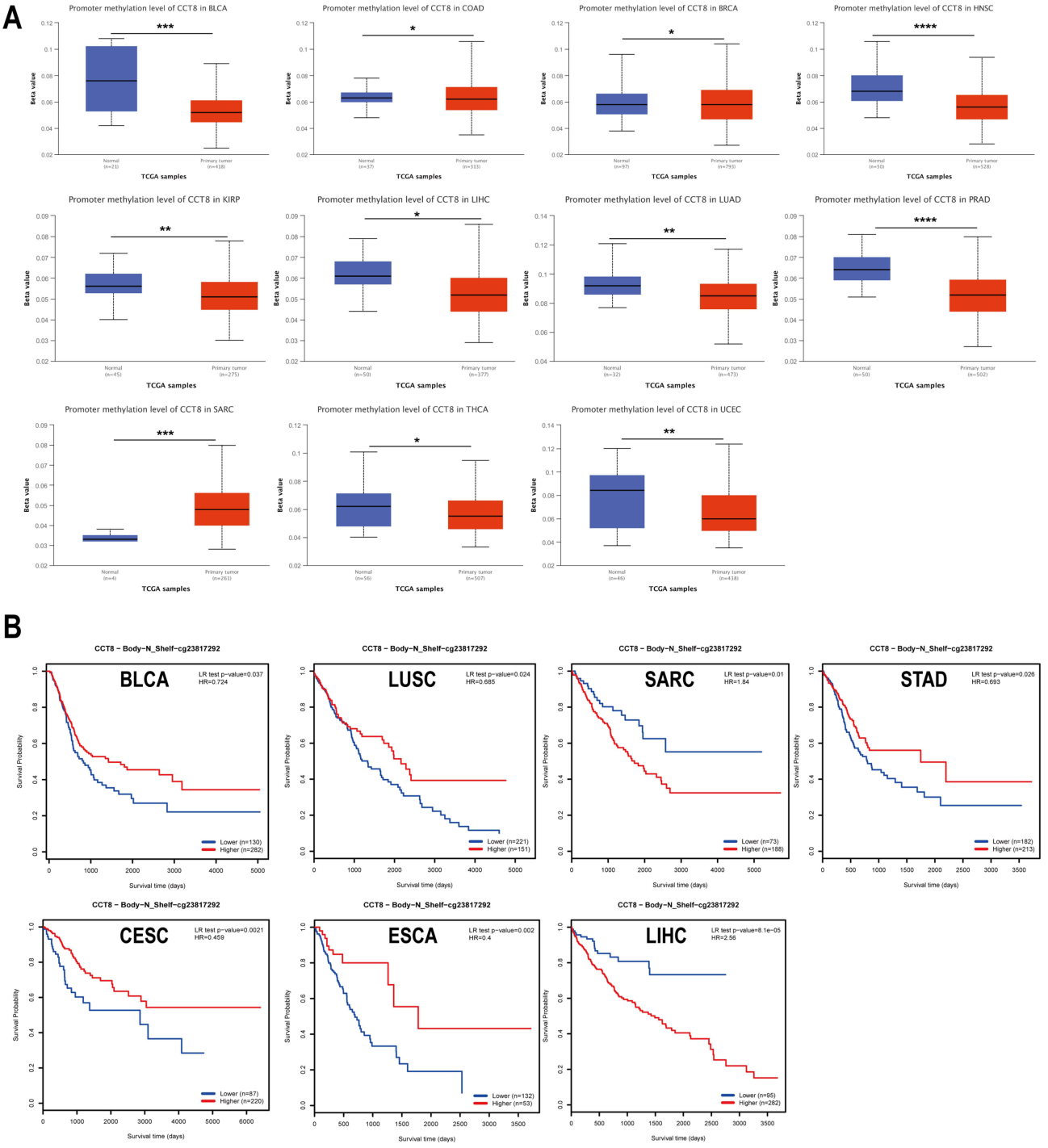

Figure 3 The promoter methylation of CCT8. (**A**) The promoter region methylation of CCT8 in cancer and paracancerous tissues was analyzed using ULCAN. (**B**) Survival curve of CCT8 methylation at cg23817292 site in various tumors. The Wilcoxon test and LR test was used for the above analysis (*p < 0.05; **p < 0.01; ***p < 0.001; ****p < 0.001).

Immune Infiltration, Immunotherapy and CCT8-Associated Drugs

The immune infiltration analysis using ESTIMATE showed that CCT8 expression was negatively correlated with the ImmuneScore, StromalScore and ESTIMATEScore in most cancers. We observed that CCT8 expression was significantly correlated with immune infiltration in 24 cancers, of which 21 were significantly negatively correlated. CCT8 had correlations of ≤-0.3 with ImmuneScore in STES, SARC, SKCM-M, SKCM-P and AC (Figure 6A); ≤-0.3 with

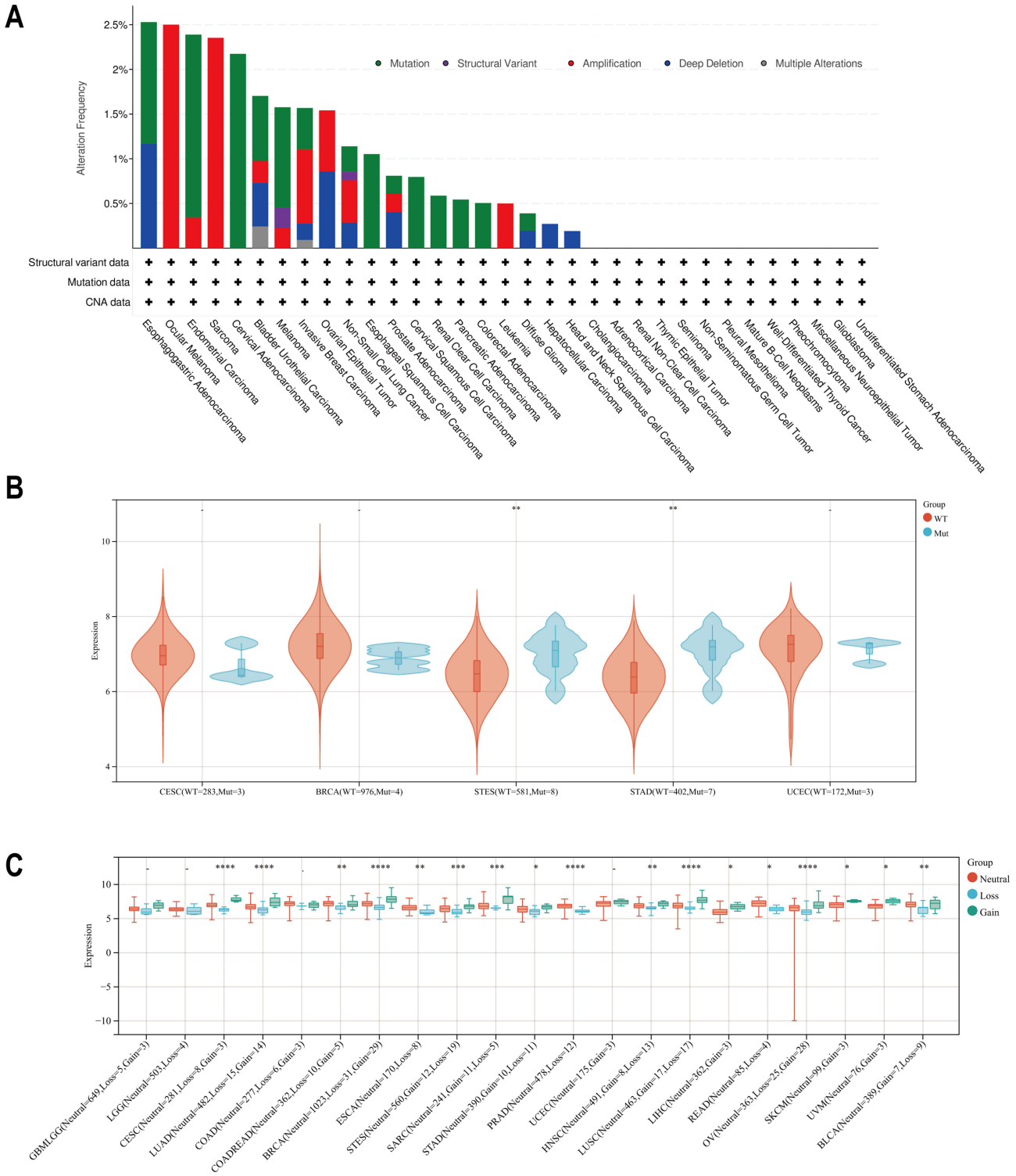

Figure 4 The genetic alteration of CCT8. (**A**) The CCT8 genetic alteration analysis in TCGA cancers was conducted by cBioPortal. The color represented the type of genetic alteration. The abscissa represented the different tumor types, and the ordinate represented the alteration frequency. (**B** and **C**) Sangerbox was used to analyze the effect of SNV (**B**) and CNV (**C**) on the CCT8 expression. In Figure (**B**), Orange represented WT and blue represented Mut. In Figure (**C**), Orange, blue, and green represented Neutral, Loss, Gain, respectively. In the (**B** and **C**) The abscissa represented different tumors, and the ordinate represented the expression level of CCT8. The Wilcoxon test was used for the above analysis (*p < 0.05; **p < 0.01; ***p < 0.001; ****p < 0.001).

StromalScore in STES, SARC, STAD, TGCT and ACC (Figure 6B); and ≤-0.3 with ImmuneScore in SARC, ACC, SKCM-M and SKCM-P (Figure 6C). Sangerbox analysis showed that CCT8 expression was negatively associated with the vast majority of immune cells, which is consistent with the ESTIMATE analysis results (Figure 6D). Interestingly,

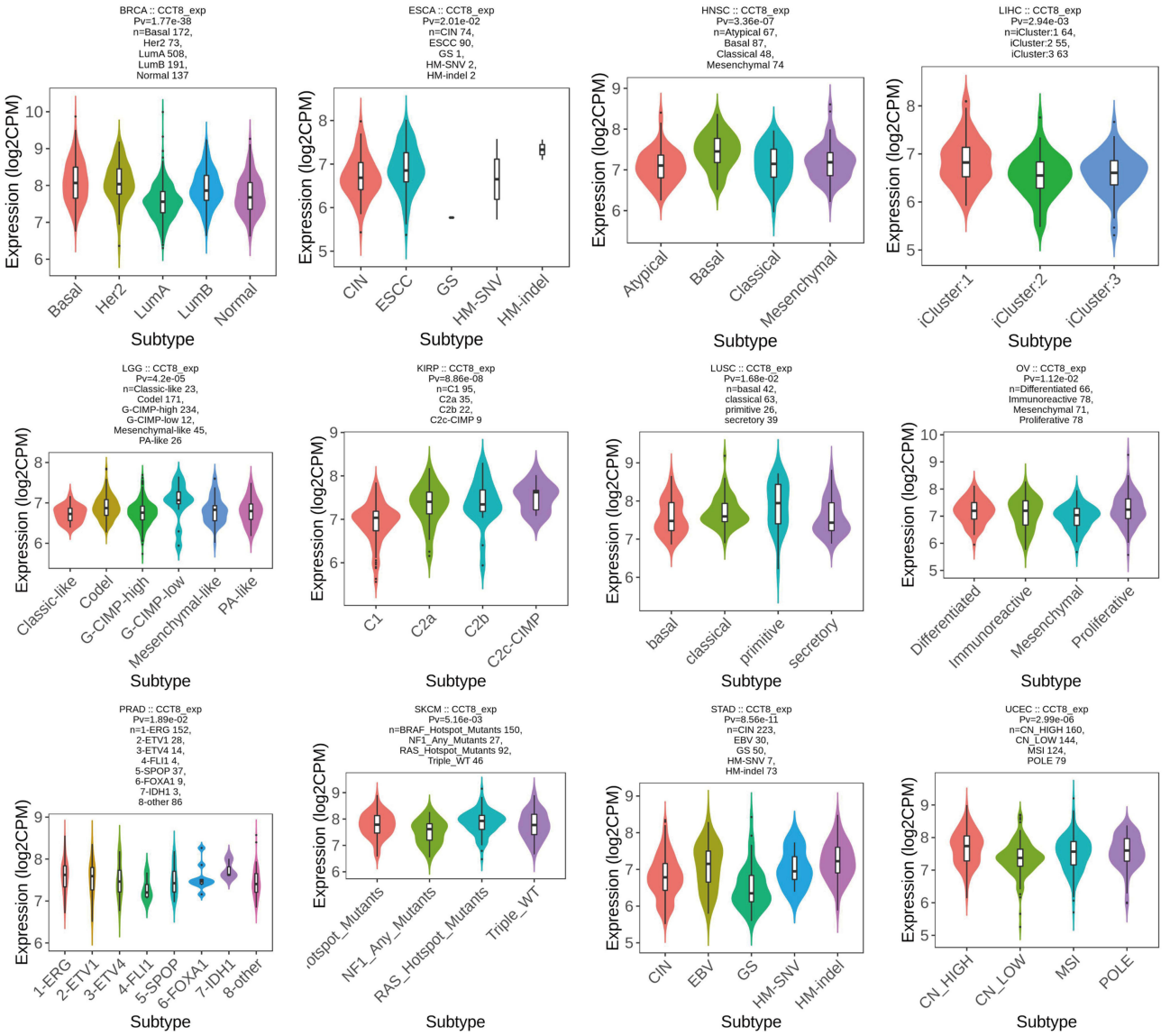

Figure 5 CCT8 expression in pan-cancer molecular subtypes. CCT8 expression in molecular subtypes of BRCA, ESCA, HNSC, KIRP, LGG, LIHC, LUSC, OV, PRAD, SKCM, STAD and UCEC. The abscissa represented various subtypes of different tumors, and the ordinate represented the CCT8 expression. The Kruskal–Wallis test was used for the above analysis.

CCT8 was positively associated with the activated CD4 T cells and type 2 T-helper cells. Furthermore, Timer showed that CCT8 was positively correlated with TH2 in many tumors (Supplementary Figure 7).

We further investigated the association between CCT8 expression and classical immune checkpoints, such as CD274, PDCD1, CTLA4, PDCD1LG2, TIGIT, HAVCR2 and LAG3 (Supplementary Figure 8A). The results show that CCT8 expression was closely related to these immune checkpoints in various cancers. Microsatellite instability (MSI), neoantigens and tumor mutation burden (TMB) could indirectly predict the efficacy of immunotherapy. It was found that CCT8 expression was positively correlated with MSI in UCEC, LIHC, SARC, STAD, KIRC, HNSC and GBM, and negatively associated in PRAD (Supplementary Figure 8B). CCT8 expression was positively correlated with neoantigens in UCEC and STAD, and positively associated with TMB in UCEC, CESC, COAD, STAD, CHOL and HNSC (Supplementary Figure 8C and D). TISMO showed that CCT8 could predict immunotherapy response in two mouse immunotherapy cohorts and five tumor cell lines (Figure 7A and B).[8] The results of CMap analysis showed that Tacrolimus and iloprost were significantly enriched in most cancers and positively correlated with CCT8 (Figure 7C).

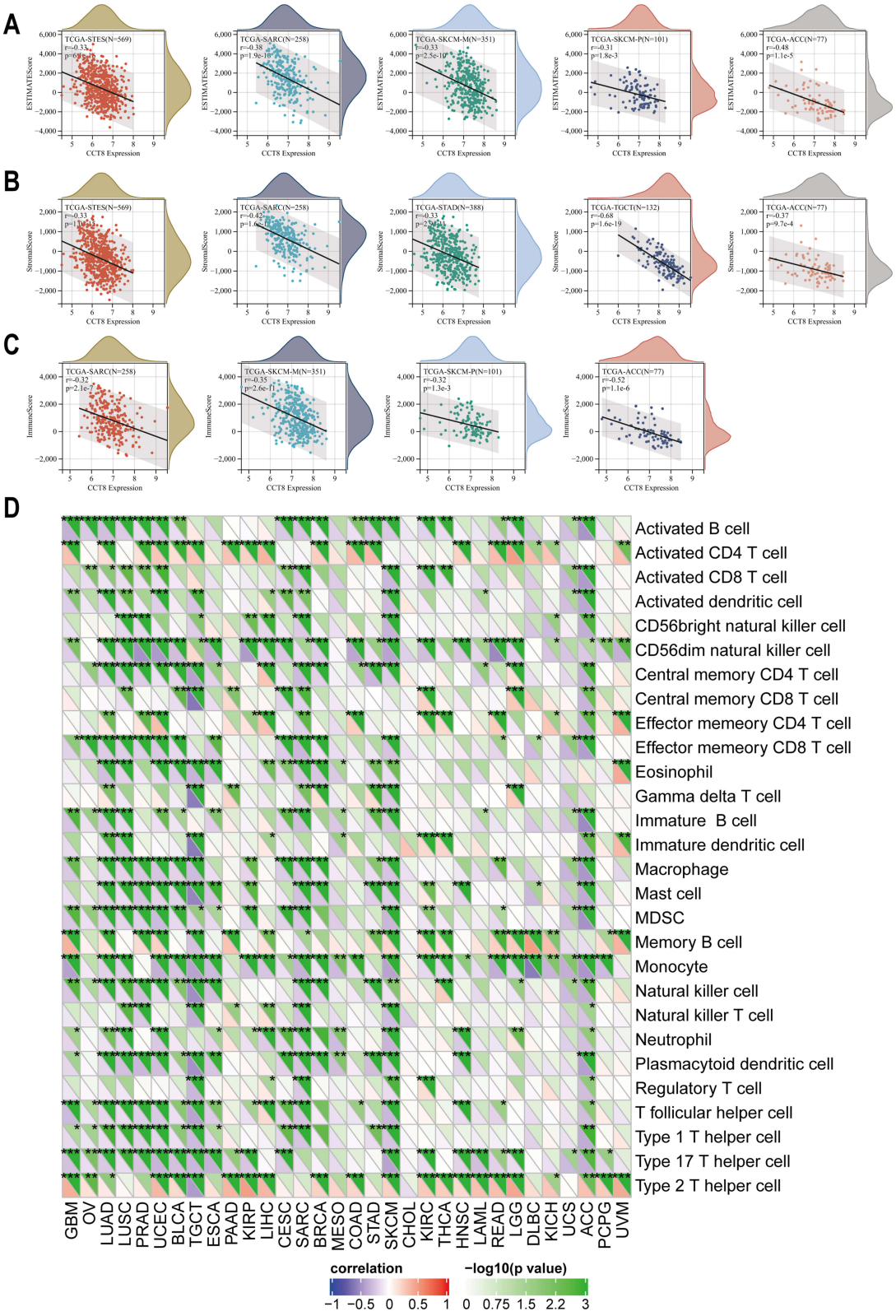

Figure 6 The correlation between CCT8 expression and immune infiltration. (**A**–**C**) The ESTIMATE analysis showed the correlation of CCT8 expression with ESTIMATEScore (**A**), StromalScore (**B**) and ImmuneScore (**C**) by ESTIMATE. The abscissa represented the CCT8 expression, and the ordinate represented the ESTIMATEScore, stromalscore and immunescore, respectively. (**D**) Sangerbox revealed the correlation between CCT8 expression and immune cells. The red and purple represented positive and negative correlations, respectively. Pearson correlation analysis was used for the above analysis (*p < 0.05; **p < 0.01; ***p < 0.001).

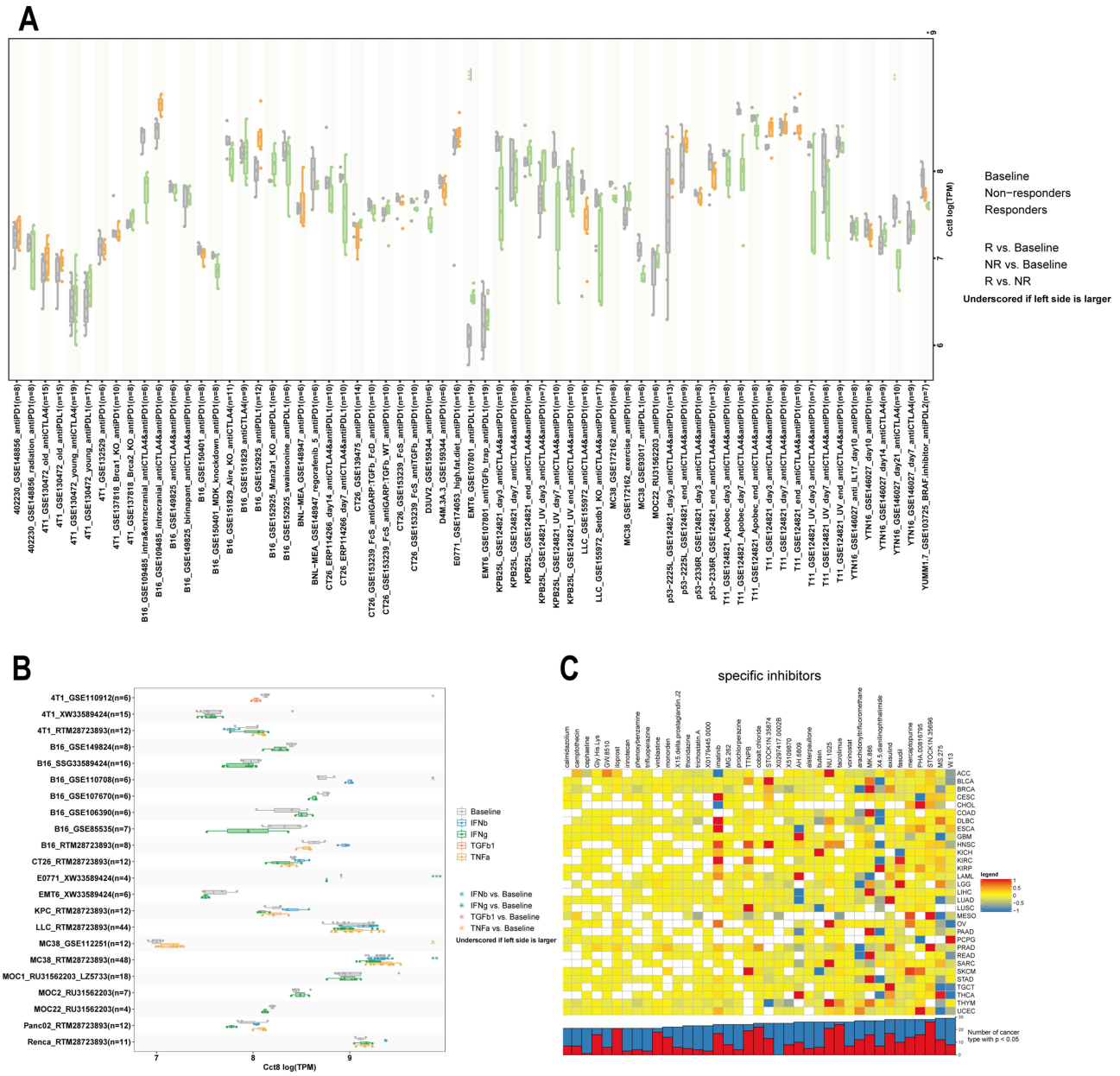

Figure 7 Immunotherapy sensitivity and associated drugs of CCT8. (**A** and **B**) TISMO showed the capability of CCT8 expression to predict immunotherapy response in mouse immunotherapy cohorts (**A**) and tumor cell lines (**B**). (**C**) Heatmap showing the enrichment fraction of different compounds in each cancer (positive in blue, negative in red). Components or drugs are listed from right to left in descending order of the number of enriched cancers. *p < 0.05; **p < 0.01; ***p < 0.001.

However, CCT8 is inversely correlated with cephaleline, irinotecan, phenoxybenzamine, trifluoperazine, thioridazine and trichostatin.A in the vast majority of various malignant tumors.

Enrichment Analysis of CCT8-Related Genes and CCT8 Functional Verification

We screened out CCT8-related genes through GEPIA and STRING for enrichment analysis to clarify the molecular mechanism of CCT8 in tumor initiation and progression. Firstly, the top 100 genes with a similar expression pattern to CCT8 in all the TCGA cancers were screened out by GEPIA, among which MIS18A, MRPL39, TCP1, MSH2, RRP1B and CDC25A were the most relevant (Figure 8A). We used STRING to obtain 48 genes that were experimentally verified to physically bind to CCT8 (Figure 8B). The Venn diagram shows there were a total of 143 genes and 5 common genes in the above two gene sets, including PDCL3, TCP1, CCT3, TRIM28 and CCT7 (Figure 8C). Go and KEGG enrichment

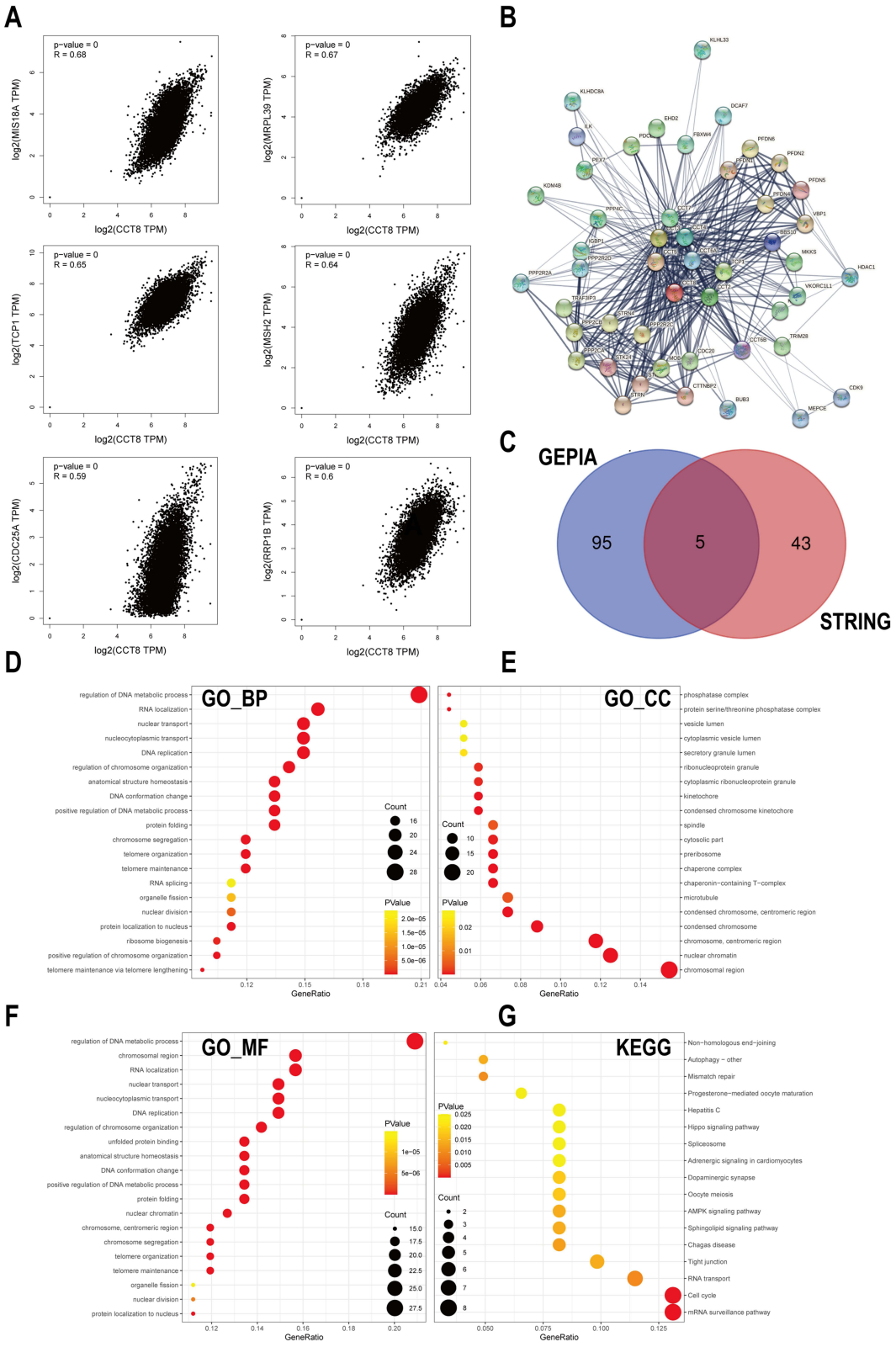

Figure 8 The enrichment analysis of CCT8-related genes. (**A**) GEPIA was used to screen out the 6 genes most closely associated with CCT8. The abscissa represented the CCT8 expression, and the abscissa represented the expression level of associated genes. (**B**) A total of 48 genes that were experimentally verified to physically bind to CCT8 were found by STRING. (**C**) The intersection of 100 genes significantly associated with CCT8 in GEPIA with 48 genes physically bound to CCT8 which was experimentally verified. (**D**–**G**) Go and KEGG enrichment analysis of 143 CCT8 related genes. The size of the dots represented the count. The redder the color of the dot, the smaller the P-value. (**A**) was analyzed via Pearson correlation analysis.

analysis were conducted for these 143 genes. The top three GO_BPs with the largest number of enriched genes were the regulation of DNA metabolic process, RNA localization and nuclear transport (Figure 8D). The top three GO_MFs were the regulation of DNA metabolic process, chromosomal region and RNA localization (Figure 8E). The top three GO_CCs were chromosomal region, nuclear chromatin and chromosomes and centromeric region (Figure 8F). The top three KEGG signaling pathways were the mRNA surveillance pathway, cell cycle and RNA transport (Figure 8G). Thus, we inferred that CCT8 plays a vital role in the cell cycle and RNA transport of cancers.

According to the above results, most cancers with highly expressed CCT8 have a poor prognosis, such as COAD, LUAD, UCEC, HNSC and LIHC. It had been demonstrated that CCT8 is highly expressed in many cancers and promotes malignant phenotypes.[2–5,24] We experimentally confirmed that the proliferation and migration of lung adenocarcinoma cells were significantly reduced after knockdown of CCT8 (Figure 9A–E), suggesting that CCT8 plays a role in promoting cancer in lung adenocarcinoma.

Discussion

Emerging evidence suggests that CCT8 promotes the proliferation and migration of colon cancer, pancreatic cancer, esophageal cancer, glioma and liver cancer, and that its expression is negatively correlated with prognosis.[2–5,24] The bioinformatics analysis and pan-cancer analysis based on public cancer datasets and repositories can help us further understand the influence of molecules on tumor occurrence and progression,[25,26] however the pan-cancer analysis of CCT8 had not been reported. Thus, we analyzed the gene expression, survival, methylation, genetic alteration and immune infiltration of CCT8 in a pan-cancer manner. We performed GO and KEGG analysis on CCT8-related genes and in vitro cell experiments to explore the potential role of CCT8 in cancer.

Our study revealed that CCT8 was highly expressed in most malignant tumors. The Cox proportional hazards regression mode and KM analysis suggested that high expression of CCT8 in a variety of cancers was negatively correlated with prognosis, which indicated that CCT8 was a good potential prognostic biomarker candidate for various cancers. It has been reported that methylation and genetic alteration in the promoter region could regulate gene expression.[23,27,28] Thus, our study investigated the promoter methylation and genetic alteration of CCT8 to explore the mechanisms behind significantly varying CCT8 expression. The results showed that the promoter region's methylation levels of CCT8 in BLCA, COAD, HNSC, KIRP, LIHC, LUAD, PRAD, THCA and UCEC were lower than in adjacent tissues, and CCT8 mRNA expression was increased in the above nine cancers. Previous studies had shown that the most common function of DNA methylation was to inactivate transcription,[23] suggesting that the reduced methylation levels in the promoter region of CCT8 might be an important cause of the up-regulation of CCT8 in cancers. cg23817292 was the most common single CpG methylation of CCT8. Cbioportal and Sangerbox were utilized to explore the effect of genetic alteration on CCT8 expression. It was found that the gain and loss groups in CNV promoted and inhibited gene expression, respectively, which suggested that CNV might be an important factor in regulating CCT8 expression.

TISIDB analysis showed that CCT8 expression affected the molecular subtype of cancers. Vésteinn et al conducted an immunogenicity analysis of 33 cancers in TCGA with over 10,000 tumor samples, dividing all non-hematological tumors into six immune subtypes, among which C3 had the best prognosis.[29] TISIDB showed that there were significant differences in CCT8 expression among the different molecular subtypes and immune subtypes in multiple tumors. It was found that CCT8 had the lowest expression in the C3 subtype with the best prognosis in most tumors, indicating that CCT8 might affect the immune infiltration of cancers. ESTIMATE estimated the ratio of immune matrix components for each sample, and presented in the form of ImmuneScore, StromalScore and ESTIMATEScore, which were positively correlated with the immune component, matrix component and the sum of the two.[30,31] The outcomes indicated that CCT8 expression was negatively associated with immune infiltration and most immune cells in the vast majority of cancers according to Sangerbox analysis. Interestingly, CCT8 was positively associated with the activated CD4 T cells and type 2 T-helper cells. Furthermore, it was found that CCT8 was positively correlated with TH2 cells in almost all cancers, according to Timer 2.0.

Bergithe's studies had shown that Th2 cell polarization and T-cell metabolism are dependent on CCT8 expression,[32] but no research has reported the effect of CCT8 on tumor-infiltrating lymphocytes (TILs). Our study firstly demonstrated that CCT8 expression was positively correlated with CD4+ Th2 cell infiltration in the vast majority of TCGA cancers.

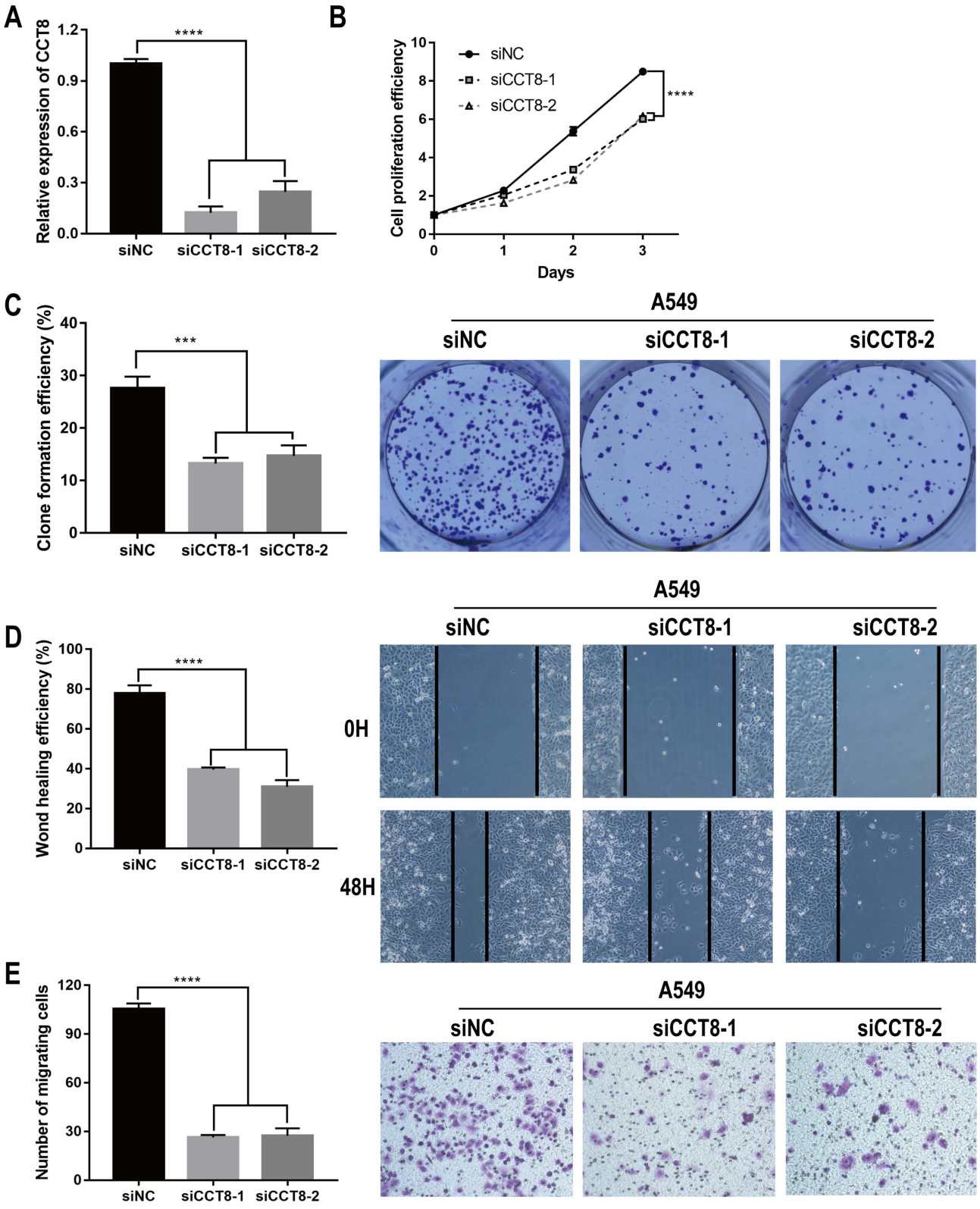

Figure 9 The functional verification of CCT8. (**A**) qRT-PCR detected the expression level of CCT8. (**B** and **C**) CCK-8 assay (**B**) and colony formation assay (**C**) showed the cell proliferation. (**D** and **E**) The wound healing assay (**D**) and Transwell assay (**E**) revealed the cell migration. ***p < 0.001; ****p < 0.0001.

TH1 and TH2 are the two main types of CD4+ T cells. TH1 polarization depends on IL-12 and IFN-γ cytokines, and TH2 polarization depends on IL-4.[33] In general, the TH1/TH2 balance plays a vital role in regulating tumor immune response, and an alteration beneficial for TH1 response brings about TH2 response dissipation and vice versa, separately leading to either anti- or pro-tumorigenic outcomes.[34–37] Takashima's research revealed that a low TH2 was associated with better OS in glioblastoma multiforme via analyzing TCGA data.[38] Researches had showed that T2 cells and T2-released cytokines elevated in many cancers.[1,39–41] It has been illustrated that maintaining a TH1-high/TH2-low balance is paramount in achieving a good prognosis for cancers. Our research might provide a new biomarker for forecasting immunotherapy response. The development of new strategies targeting CCT8 might benefit to correct Th1/Th2 imbalance and improve prognosis in patients with high CCT8 expression. We screened many CCT8-related anticancer inhibitors by CMap analysis, including irinotecan, a cytotoxic drug that has been widely used in the treatment of metastatic or advanced solid tumors.

To explore the molecular mechanism of CCT8 in regulating tumorigenesis and development in cancer, we obtained 143 molecules that had similar expression patterns or were physically bound to CCT8 through GEPIA and STRING, and then carried out GO and KEGG analysis, which showed that CCT8 plays a vital role in the cell cycle and RNA transport of cancers. Based on the above results, CCT8 is highly expressed in most malignant tumors, such as COAD, LUAD, UCEC, HNSC and liver cancer, and negatively correlated with prognosis. It has been demonstrated that CCT8 is highly expressed in many cancers and promotes malignant phenotypes.[2,4,5,24,29] However, there has been no study exploring the role of CCT8 in lung adenocarcinoma. We experimentally confirmed that the proliferation and migration of lung adenocarcinoma cells were significantly reduced after knockdown of CCT8, suggesting that CCT8 played a role in promoting cancer in lung adenocarcinoma.

Although we performed a comprehensive and systematic analysis of CCT8 and cross-validated it using different databases and experiments, there are some limitations in our study. Our study verified that CCT8 promoted tumorigenesis and development only in LUAD, and the role of CCT8 in other tumors still needed to be explored. Although our results suggested that CCT8 expression was closely associated with immune infiltration and poor prognosis of cancers, it was short of direct evidence that high CCT8 lead to poor prognosis by immune infiltration. Although we identified potential drugs associated with CCT8 through CMAP analysis, more experiments were still needed to further explore the evidence of direct interaction between CCT8 and these components. Therefore, in the future, we will supplement experiments to verify the effect of CCT8 on immune infiltration and immunotherapy, and explore the mechanism of CCT8 participating in immune regulation.

Conclusion

In conclusion, our study firstly and comprehensively analyzed CCT8 in a pan-cancer manner. The results indicate that CCT8 is highly expressed in most cancers, correlates with poor prognosis and promotes the proliferation and migration of cancers. The results also suggest that CCT8 might be a biomarker of CD4+ Th2 cell infiltration and a promising therapeutic target for Th1/Th2 imbalance.

Abbreviations

CCT8, Chaperonin containing TCP1 subunit 8; GO, Gene Ontology; KEGG, Kyoto Encyclopedia of Genes and Genomes; TCGA, The Cancer Genome Atlas; GTEx, The Genotype-Tissue Expression; CPTAC, Clinical Proteomic Tumor Analysis Consortium; ICPC, International Cancer Proteogenome Consortium; OS, overall survival; DFS, disease free survival; DSS, disease specific survival; DFI, disease free interval; PFI, progression free interval; Th2, T-helper type 2; Th1, T-helper type 1; CNV, Copy Number Variation; SNV, Single Nucleotide Variants; MSI, microsatellite instability; TMB, tumor mutation burden; ACC, adrenocortical carcinoma; BLCA, bladder urothelial carcinoma; BRCA, breast invasive carcinoma; CESC, cervical squamous cell carcinoma and endocervical adenocarcinoma; CHOL, cholangiocarcinoma; COAD, colon adenocarcinoma; DLBC, lymphoid neoplasm diffuse large B-cell lymphoma; ESCA, esophageal carcinoma; GBM, glioblastoma multiforme; HNSC, head and neck squamous cell carcinoma; KICH, kidney chromophobe; KIRC, kidney renal clear cell carcinoma; KIRP, kidney renal papillary cell carcinoma; LGG, brain lower grade glioma; LIHC, liver hepatocellular carcinoma; LUAD, lung adenocarcinoma; LUSC, lung squamous cell carcinoma;

MESO, mesothelioma; OV, ovarian serous cystadenocarcinoma; PAAD, pancreatic adenocarcinoma; PCPG, pheochromocytoma and paraganglioma; PRAD, prostate adenocarcinoma; READ, rectum adenocarcinoma; SARC, sarcoma; SKCM, skin cutaneous melanoma; STAD, stomach adenocarcinoma; TGCT, testicular germ cell tumours; THCA, thyroid carcinoma; THYM, thymoma; UCEC, uterine corpus endometrial carcinoma; UCS, uterine carcinosarcoma; UVM, uveal melanoma.

Data Sharing Statement

The original contributions presented in the study are included in the article/Supplementary Material. Further inquiries can be directed to the corresponding authors.

Ethics Statement

All experiments and methods were performed in accordance with the relevant approved guidelines and regulations, as well as under the approval of the Ethics Committee of the Third Xiangya Hospital of Central South University (No. I 22277).

Acknowledgments

We acknowledge the TCGA, CPTAC, ICPC, GTEx, cBioPortal, UALCAN, TISIDB, Sangerbox and Human Protein Atlas websites for providing their platforms and meaningful datasets. We also sincerely thank the Central Laboratory of the Third Xiangya Hospital and all participants involved in this study.

Author Contributions

All authors made significant contributions to the conception and design, acquisition of data, or analysis and interpretation of data; participated in drafting the article or critically revising important intellectual content; agreed to submit the article to the current journal; gave final approval of the version to be published; and agreed to take responsibility for all aspects of the work.

Funding

This work was supported by the Funds for International Cooperation and Exchange of the National Natural Science Foundation of China (GZ1699), key research and development projects in Hunan Province (2022SK2022), the science and technology innovation Program of Hunan Province (2020RC4011), the Hunan Province Science and Technology Talent Promotion Project (2019TJ-Q10), Scientific research project of Hunan Provincial Health Commission (202209034683), Young Scholars of "Furong Scholar Program" in Hunan Province, Central South University Research Programme of Advanced Interdisciplinary Studies (2023QYJC017), and the Wisdom Accumulation and Talent Cultivation Project of the Third xiangya hospital of Central South University (BJ202001).

Disclosure

The authors declare that the research was conducted in the absence of any commercial or financial relationships that could be construed as a potential conflict of interest.

References

1. Qin H, Lu Y, Du L, et al. Pan-cancer analysis identifies LMNB1 as a target to redress Th1/Th2 imbalance and enhance PARP inhibitor response in human cancers. *Cancer Cell Int*. 2022;22:101. doi:10.1186/s12935-022-02467-4
2. Liao Q, Ren Y, Yang Y, et al. CCT8 recovers WTp53-suppressed cell cycle evolution and EMT to promote colorectal cancer progression. *Oncogenesis*. 2021;10:84. doi:10.1038/s41389-021-00374-3
3. Yang X, Ren H, Shao Y, et al. Chaperonin-containing T-complex protein 1 subunit 8 promotes cell migration and invasion in human esophageal squamous cell carcinoma by regulating α-actin and β-tubulin expression. *Int J Oncol*. 2018;52(6):2021–2030. doi:10.3892/ijo.2018.4335
4. Qiu X, He X, Huang Q, et al. Overexpression of CCT8 and its significance for tumor cell proliferation, migration and invasion in glioma. *Pathol Res Pract*. 2015;211:717–725. doi:10.1016/j.prp.2015.04.012
5. Huang X, Wang X, Cheng C, et al. Chaperonin containing TCP1, subunit 8 (CCT8) is upregulated in hepatocellular carcinoma and promotes HCC proliferation. *APMIS*. 2014;122:1070–1079. doi:10.1111/apm.12258

6. Cui X, Zhang X, Liu M, et al. A pan-cancer analysis of the oncogenic role of staphylococcal nuclease domain-containing protein 1 (SND1) in human tumors. *Genomics*. 2020;112:3958–3967. doi:10.1016/j.ygeno.2020.06.044
7. Fang Z, Li P, Li H, et al. New insights into PTBP3 in human cancers: immune cell infiltration, TMB, MSI, PDCD1 and m6A markers. *Front Pharmacol*. 2022;13:811338. doi:10.3389/fphar.2022.811338
8. Wei C, Wang B, Peng D, et al. Pan-cancer analysis shows that ALKBH5 is a potential prognostic and immunotherapeutic biomarker for multiple cancer types including gliomas. *Front Immunol*. 2022;13:849592. doi:10.3389/fimmu.2022.849592
9. Chen AS, Wardwell-Ozgo J, Shah NN, et al. Drak/STK17A drives neoplastic glial proliferation through modulation of MRLC signaling. *Cancer Res*. 2019;79:1085–1097. doi:10.1158/0008-5472.CAN-18-0482
10. Gao L, Zhang W, Zhang J, et al. KIF15-mediated stabilization of AR and AR-V7 contributes to enzalutamide resistance in prostate cancer. *Cancer Res*. 2021;81:1026–1039. doi:10.1158/0008-5472.CAN-20-1965
11. Tang Z, Kang B, Li C, Chen T, Zhang Z. GEPIA2: an enhanced web server for large-scale expression profiling and interactive analysis. *Nucleic Acids Res*. 2019;47:W556–W60. doi:10.1093/nar/gkz430
12. Uhlen M, Fagerberg L, Hallstrom BM, et al. Proteomics. Tissue-based map of the human proteome. *Science*. 2015;347:1260419. doi:10.1126/science.1260419
13. Barretina J, Caponigro G, Stransky N, et al. The cancer cell line encyclopedia enables predictive modelling of anticancer drug sensitivity. *Nature*. 2012;483:603–607. doi:10.1038/nature11003
14. Kao T-J, Wu -C-C, Phan NN, et al. Prognoses and genomic analyses of proteasome 26S subunit, ATPase (PSMC) family genes in clinical breast cancer. *Aging*. 2021;13:17970. doi:10.18632/aging.203345
15. Li W, Ma J-A, Sheng X, Xiao C. Screening of CXC chemokines in the microenvironment of ovarian cancer and the biological function of CXCL10. *World J Surg Oncol*. 2021;19:329. doi:10.1186/s12957-021-02440-x
16. Modhukur V, Iljasenko T, Metsalu T, Lokk K, Laisk-Podar T, Vilo J. MethSurv: a web tool to perform multivariable survival analysis using DNA methylation data. *Epigenomics*. 2018;10:277–288. doi:10.2217/epi-2017-0118
17. Anuraga G, Wang W-J, Phan NN, et al. Potential prognostic biomarkers of NIMA (Never in Mitosis, Gene A)-Related Kinase (NEK) family members in breast cancer. *J Pers Med*. 2021;11:1089. doi:10.3390/jpm11111089
18. Song Y, Ma R. Identifying the potential roles of PBX4 in human cancers based on integrative analysis. *Biomolecules*. 2022;12:822. doi:10.3390/biom12060822
19. Zhong M, Wang X, Zhu E, et al. Analysis of pyroptosis-related immune signatures and identification of pyroptosis-related LncRNA prognostic signature in clear cell renal cell carcinoma. *Front Genet*. 2022;13:905051. doi:10.3389/fgene.2022.905051
20. Subramanian A, Narayan R, Corsello SM, et al. A next generation connectivity map: L1000 Platform and the First 1,000,000 Profiles. *Cell*. 2017;171:1437–1452.e17. doi:10.1016/j.cell.2017.10.049
21. Wang C-Y, Chiao -C-C, Phan NN, et al. Gene signatures and potential therapeutic targets of amino acid metabolism in estrogen receptor-positive breast cancer. *Am J Cancer Res*. 2020;10:95–113.
22. Tu Z, Peng J, Long X, et al. Sperm autoantigenic protein 17 predicts the prognosis and the immunotherapy response of cancers: a pan-cancer analysis. *Front Immunol*. 2022;13:844736. doi:10.3389/fimmu.2022.844736
23. Jones PA. Functions of DNA methylation: islands, start sites, gene bodies and beyond. *Nat Rev Genet*. 2012;13:484–492. doi:10.1038/nrg3230
24. Liu P, Kong L, Jin H, Wu Y, Tan X, Song B. Differential secretome of pancreatic cancer cells in serum-containing conditioned medium reveals CCT8 as a new biomarker of pancreatic cancer invasion and metastasis. *Cancer Cell Int*. 2019;19:262. doi:10.1186/s12935-019-0980-1
25. Li J, Xie J, Wu D, et al. A pan-cancer analysis revealed the role of the SLC16 family in cancer. *Channels*. 2021;15:528–540. doi:10.1080/19336950.2021.1965422
26. Xie J, Ruan S, Zhu Z, et al. Database mining analysis revealed the role of the putative H+/sugar transporter solute carrier family 45 in skin cutaneous melanoma. *Channels*. 2021;15:496–506. doi:10.1080/19336950.2021.1956226
27. Chen S, Li K, Cao W, et al. Codon-resolution analysis reveals a direct and context-dependent impact of individual synonymous mutations on mRNA level. *Mol Biol Evol*. 2017;34:2944–2958. doi:10.1093/molbev/msx229
28. Stranger BE, Forrest MS, Dunning M, et al. Relative impact of nucleotide and copy number variation on gene expression phenotypes. *Science*. 2007;315:848–853. doi:10.1126/science.1136678
29. Thorsson V, Gibbs DL, Brown SD, et al. The Immune Landscape of Cancer. *Immunity*. 2018;48:812–30 e14. doi:10.1016/j.immuni.2018.03.023
30. Aran D, Sirota M, Butte AJ. Systematic pan-cancer analysis of tumour purity. *Nat Commun*. 2015;6:8971. doi:10.1038/ncomms9971
31. Yoshihara K, Shahmoradgoli M, Martinez E, et al. Inferring tumour purity and stromal and immune cell admixture from expression data. *Nat Commun*. 2013;4:2612. doi:10.1038/ncomms3612
32. Oftedal BE, Maio S, Handel AE, et al. The chaperonin CCT8 controls proteostasis essential for T cell maturation, selection, and function. *Commun Biol*. 2021;4:681. doi:10.1038/s42003-021-02203-0
33. Basu A, Ramamoorthi G, Albert G, et al. Differentiation and Regulation of TH cells: a balancing act for cancer immunotherapy. *Front Immunol*. 2021;12:669474. doi:10.3389/fimmu.2021.669474
34. Saravia J, Chapman NM, Helper CH. T cell differentiation. *Cell Mol Immunol*. 2019;16:634–643. doi:10.1038/s41423-019-0220-6
35. Zhang S, Nguyen LH, Zhou K, et al. Knockdown of anillin actin binding protein blocks cytokinesis in hepatocytes and reduces liver tumor development in mice without affecting regeneration. *Gastroenterology*. 2018;154:1421–1434. doi:10.1053/j.gastro.2017.12.013
36. Dobrzanski MJ. Expanding roles for CD4 T cells and their subpopulations in tumor immunity and therapy. *Front Oncol*. 2013;3:63. doi:10.3389/fonc.2013.00063
37. Luckheeram RV, Zhou R, Verma AD, Xia B. CD4(+)T cells: differentiation and functions. *Clin Dev Immunol*. 2012;2012:925135. doi:10.1155/2012/925135
38. Takashima Y, Kawaguchi A, Kanayama T, Hayano A, Yamanaka R. Correlation between lower balance of Th2 helper T-cells and expression of PD-L1/PD-1 axis genes enables prognostic prediction in patients with glioblastoma. *Oncotarget*. 2018;9:19065–19078. doi:10.18632/oncotarget.24897
39. Maier B, Leader AM, Chen ST, et al. A conserved dendritic-cell regulatory program limits antitumour immunity. *Nature*. 2020;580:257–262. doi:10.1038/s41586-020-2134-y

40. Mahata B, Zhang X, Kolodziejczyk AA, et al. Single-cell RNA sequencing reveals T helper cells synthesizing steroids de novo to contribute to immune homeostasis. *Cell Rep*. 2014;7:1130–1142. doi:10.1016/j.celrep.2014.04.011
41. DeNardo DG, Barreto JB, Andreu P, et al. CD4(+) T cells regulate pulmonary metastasis of mammary carcinomas by enhancing protumor properties of macrophages. *Cancer Cell*. 2009;16:91–102. doi:10.1016/j.ccr.2009.06.018